

# Neuronal impedance mechanism implementing cooperative networks with low firing rates and $\mu$ s precision

Roni Vardi<sup>1†</sup>, Hagar Marmari<sup>1†</sup>, Amir Goldental<sup>2†</sup>, Haya Brama<sup>1</sup>, Edward Stern<sup>1,3</sup>, Shira Sardi<sup>1,2</sup>, Pinhas Sabo<sup>1,2</sup> and Ido Kanter<sup>1,2,\*</sup>

<sup>1</sup>Gonda Interdisciplinary Brain Research Center, Bar-Ilan University, Ramat-Gan 52900, Israel

<sup>2</sup>Department of Physics, Bar-Ilan University, Ramat-Gan 52900, Israel

<sup>3</sup>Institute for Neurodegenerative Disease, Department of Neurology, Massachusetts General Hospital, MA, USA

†These authors contributed equally to this work.

\*Correspondence: ido.kanter@biu.ac.il

Realizations of low firing rates in neural networks usually require globally balanced distributions among excitatory and inhibitory links, while feasibility of temporal coding is limited by neuronal millisecond precision. We experimentally demonstrate  $\mu$ s precision of neuronal response timings under low stimulation frequencies, whereas moderate frequencies result in a chaotic neuronal phase characterized by degraded precision. Above a critical stimulation frequency, which varies among neurons, response failures were found to emerge stochastically such that the neuron functions as a low pass filter, saturating the average inter-spike-interval. This intrinsic neuronal response impedance mechanism, as opposed to links distribution, counter-intuitively leads to cooperation on a network level, such that firing rates are suppressed towards the lowest neuronal critical frequencies simultaneously with neuronal  $\mu$ s precision.

The attempt to understand high cognitive functionalities and cooperative activities of neurons within a network results in many open questions. One question is what mechanism underlies the extremely low firing rates, few Hertz, of neurons comprising a network of threshold units, as a single neuron is capable of much higher firing frequencies[1-3]. The rate of evoked spikes in an excitatory network is expected to increase constantly if each neuron excites several other neurons. This spike birth trend is moderated by a death trend, eliminating spikes by inhibitory synapses or weakening excitatory synapses to be sub-threshold[4]. In case the birth and death trends are not precisely balanced, the network firing rate either diverges toward extremely high firing frequencies or practically vanishes[5]. This balance can be theoretically achieved by several predefined synaptic designs depending on the topology of the network, such as a wide distribution of excitatory synaptic strengths balanced by a fraction of inhibitory synapses[6,7] or by modular networks[8,9], resulting in alternating firing.

A second puzzle is the realization of temporal coding on a network level[10,11], which is limited by the least precise building block of the network, i.e. neurons or synapses. Synaptic conductance is reproducible with accuracy of dozens of  $\mu$ s[12,13], which is meaningful only if the temporal precision of a neuron is comparable. However, the variations of the neuronal response timings are typically in the order of several ms[14,15], and are expected to accumulate to dozens of ms in chains and networks[16,17], hence questioning the feasibility of temporal coding.

In this work we demonstrate that network low firing rates and neuronal precise response timings both stem from a single neuron property, the neuronal impedance mechanism, which counter-intuitively leads to cooperation among

individual neurons comprising a network. The global features of network dynamics are governed by the distribution tail of the nodal properties rather than by specific distributions of the network links.

Neuronal precision can be experimentally determined by the neuronal response latency (NRL), which reflects the internal dynamics of the neuron and is measured as the time-lag between a stimulation and its corresponding evoked spike[18,19]. This quantity dynamically varies by several ms [16,17], as exemplified in Fig. 1(a) using cultured cortical neurons functionally separated from their network by synaptic blockers[20].

The accumulated stretching over few hundreds of repeated stimulations is typically several ms, comparable with the initial NRL. This stretching terminates at the intermittent phase, where the average NRL,  $\langle \text{NRL} \rangle = L_C$ , remains constant and is accompanied by both large fluctuations that can exceed 1 ms and a non-negligible fraction of neuronal response failures (Fig. 1(a)). The NRL increase is a fully reversible phenomenon over several seconds without stimulations.

The proof of concept for NRL stabilization is examined first under an adaptive external feedback scenario (Fig. 1(b)). It relies on the fact that the average stretching of the NRL per stimulation increases with the decrease of the time-lag,  $\tau$ , between stimulations, and vice versa[18]. Accordingly, the following real-time adaptive algorithm,  $\tau(i+1) = \tau(i) + \Delta \cdot \text{sign}[L_{ST} - L(i)]$  (Fig. 1(b)), for stabilization around a predefined NRL,  $L_{ST}$ , was experimentally tested.  $L(i)$  stands for the NRL corresponding to the  $i^{\text{th}}$  stimulation,  $\tau(i)$  stands for the time-lag between consecutive stimulations  $i-1$  and  $i$ ,  $\text{sign}$  is the signum function and  $\Delta = 20$  ms is a predefined constant, which in advanced algorithms can be

adjusted following the history,  $\{L(j)\}$ . Results indicate a supreme stabilization measured by the standard deviation  $\sigma \sim 16 \mu\text{s}$  over the last 1000 stimulations,  $\sigma/L < 10^{-2}$  (Fig. 1(c)). In order to maintain stabilization around  $L_{ST}$ ,  $\tau$  was adjusted continuously; however,  $\langle \tau \rangle$  stabilizes around 200 ms.

This proof of concept for NRL stabilization, calls for a more natural realization of this phenomenon without adaptive external control. Using a fixed  $\tau \sim 198.2$  ms,  $L_{ST} \sim 5$  ms is obtained, with  $\sigma \sim 14 \mu\text{s}$ , however the transient to stabilization is longer (Fig. 1(c)). Results suggest that the stabilized NRL,  $L_{ST}$ , is primarily a function of  $\langle \tau \rangle$ . This was confirmed through a more realistic scenario where the neuron was stimulated following random  $\tau(i)$  characterized by  $\langle \tau \rangle \sim 200$  ms, resulting in  $L_{ST}$  with a slightly larger  $\sigma$  (Fig. 1(c)).

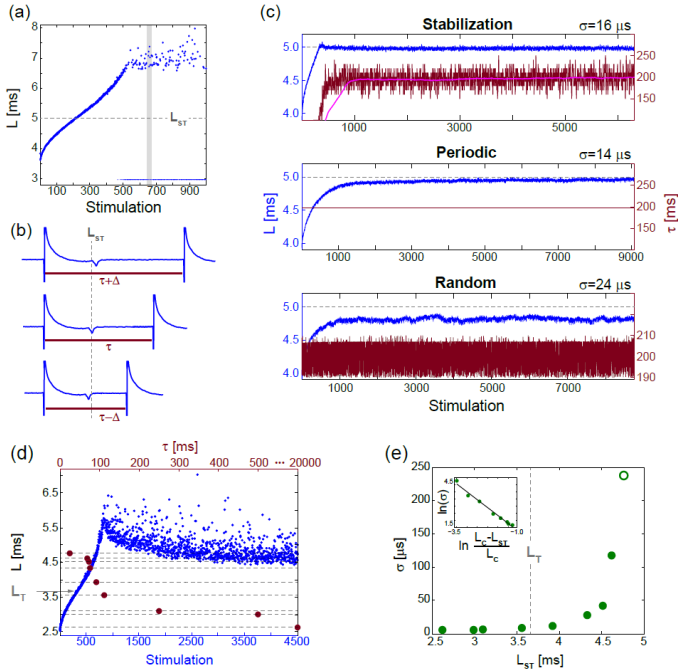


FIG. 1 (color online). (a) The response latency,  $L$ , (blue dots) of a neuron stimulated at 30 Hz, with a guideline for  $L_{ST} = 5$  ms (gray dashed-line). Response failures (blue circles) are denoted at  $L = 3$  ms. (b) Schematic of a real-time adaptive algorithm for stabilization at  $L_{ST}$ . (c) Stabilization of  $L$  (blue) at  $L_{ST} \sim 5$  ms and  $\tau$  (crimson) for: the adaptive algorithm (upper panel),  $\tau$  smoothed using 1000 stimulation sliding window (pink), periodic stimulation (middle panel) and  $\tau$  taken randomly from  $U(190, 210)$  ms (lower panel). Denoted  $\sigma$  is obtained from the last 1000 stimulations. (d)  $L$  of a neuron stimulated at 40 Hz (blue), response failures not shown, and  $L_{ST}$  (dashed-lines) as a function of  $\tau$  (crimson dots),  $L_T = 3.66$  ms. (e)  $\sigma(L_{ST})$  marked in (d) and for  $L_{ST} = L_C = 4.73$  ms (green circle). Inset: a linear fit for  $\ln(\sigma)$  versus  $\ln[(L_C - L_{ST})/L_C]$ ;  $\ln(\sigma) = -1.11 \cdot \ln[(L_C - L_{ST})/L_C] + 0.67$ .

Stabilization close to the initial NRL requires  $\tau$  in the order of seconds which rapidly decreases to  $\sim [50, 150]$  ms while approaching  $L_C$  (Fig. 1(d)). These two regions are also reflected in the behavior of  $\sigma(L_{ST})$ , where below a certain NRL,  $\sigma$  is almost constant while diverging as a power-law as  $L_C$  is approached (Fig. 1(e)). The exponent characterizing the power-law varies much among neurons. Quantitatively, the

NRL at the transition between the regions of semi-constant and rapidly increasing  $\sigma$ ,  $L_T$ , is estimated at high stimulation frequency, where the NRL profile changes its concave form to convex,  $d^2L/d\text{Stimulation}^2 = 0$ . This concave profile,  $L < L_T$ , was recently also found to identify a reproducible non-chaotic neuronal phase[21], where deviations between NRL profiles, obtained in different stimulation trials consisting of identical stimulation patterns, do not increase with the number of stimulations[21] and diverge exponentially for a chaotic neuronal phase,  $L > L_T$ .

The minimal  $\sigma$  of few  $\mu\text{s}$ , i.e.  $\sim 5 \mu\text{s}$  (Fig. 1(e)), is measured when  $L_{ST}$  is close to the initial NRL. It requires sub-Hertz stimulation rate and saturates our experimental lower bound of  $\sigma$ , which stems from the unavoidable amplified noise measured by the electrode. To overcome these limitations, we turn to the following theoretical argument. The number of ions in an evoked spike can be estimated from the density of the neuronal membrane capacitance[22]  $\sim 1 \mu\text{F}/\text{cm}^2$ . Hence, for the diameter of a typical neuronal soma[23],  $\sim 20 \mu\text{m}$  ( $\sim 10^3 \mu\text{m}^2$  surface area), one finds  $C \sim 10^{-11}$  F membrane capacitance. Using the voltage difference in the membrane during an evoked spike[22],  $\Delta V \sim 0.1$  V, the number of ions in an evoked spike scales as  $Q = C\Delta V \sim 10^7 e$ . These ions are evoked in about 1 ms, the duration of a spike, implying that an individual ion is evoked on the average every  $1 \text{ms}/10^7 = 10^{-10}$  s. Assuming a simple stochastic process for the sequential emission of ions, the expected time deviation for an evoked spike is  $\Delta t \sim 10^{-10} \cdot 10^{7/2} \sim 0.3 \mu\text{s}$ , which is only slightly below the experimentally demonstrated  $\sigma$  of extremely few  $\mu\text{s}$ .

The NRL stabilization, with fluctuations in the order of 100  $\mu\text{s}$ , was confirmed also in *in vivo* experiments, which strongly support the temporal robustness of signal transmission in the brain[24], even in cases where both synaptic and neuronal transmission are involved.

Above a critical stimulation frequency,  $f_C$ , the neuron enters the intermittent phase[19] (Fig. 2(a)). Specifically, approaching  $f_C$  from below,  $L_C$  is first achieved accompanied by large  $\sigma$  but with a vanishing fraction of response failures,  $P_{\text{fail}}$  (Fig. 2(b)). In addition, the transient time to a stationary  $\sigma$  is much enhanced (Fig. 2(b)), together with a power-law divergence of  $\sigma$  (Fig. 1(e), inset), as expected in such a second order phase transition.

Above  $f_C$ , neuronal response failures stochastically emerge with a probability  $P_{\text{fail}} \sim (\tau_C - \tau)/\tau_C$  (Fig. 2(c)). Consequently, a global tenable quantity, the average inter-spike-interval (ISI), is preserved and is equal to  $\tau/(1 - P_{\text{fail}}) \sim \tau_C$  (Fig. 2(c)), hence the neuron functions similar to a low pass filter. The stochastic occurrence of response failures was quantitatively examined by the comparison of the probability for the occurrence of all combinations of responses to their expected

values under the assumption of random uncorrelated response failures with a given  $P_{\text{fail}}$  (Fig. 2(d)). The second test consists of calculating the probabilities,  $P_0(m)$  [ $P_1(m)$ ], for the occurrence of segments of  $m$  consecutive response failures [spikes] bounded by evoked spikes [response failures]. These probabilities were found to be in a good agreement with the theoretically predicted ones based on such a Poissonian process with a rate  $-\ln(P_{\text{fail}})$  [ $-\ln(1-P_{\text{fail}})$ ] (Figs. 2(e)-2(f)).

The saturated neuronal firing frequency,  $f_C$ , functions as an impedance mechanism limiting the average firing rate. Typically,  $f_C$  is in the range of 6-15 Hz, but can be extended for some neurons as high as 27 Hz and as low as 3 Hz.

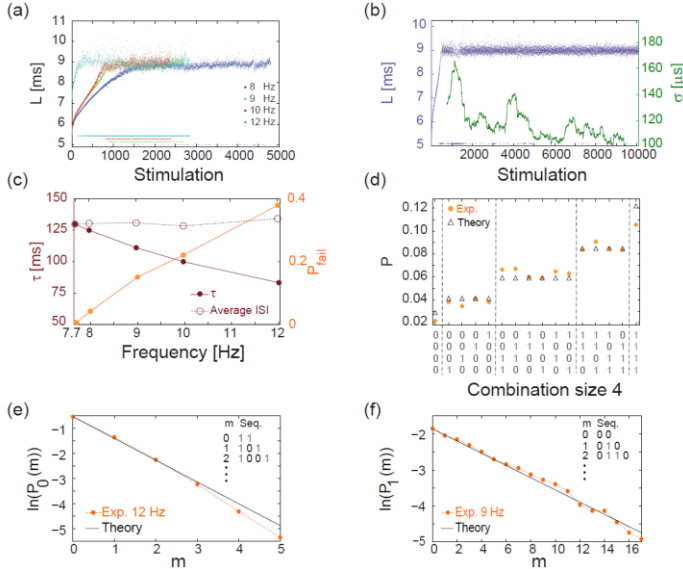


FIG. 2 (color online). (a) The response latency,  $L$ , of a neuron stimulated at 8 (blue), 9 (green), 10 (red) and 12 (cyan) Hz with corresponding  $\langle L \rangle$  over the last 1000 stimulations 8.905, 9.007, 9.062, 8.964 ms ( $L_C \sim 9$  ms). Response failures are denoted below  $L=6$  ms. (b) The neuron shown in (a) stabilized using the real-time adaptive algorithm (Fig. 1(b)) with  $L_{S\tau}=9$  ms, resulting in  $\tau \sim 130$  ms ( $\sim 7.7$  Hz). Response failures are denoted at  $L \sim 5$  ms.  $\sigma$  is smoothed using 500 stimulation sliding window (green). (c)  $P_{\text{fail}}$  (orange dots), and the corresponding  $\tau$  (crimson dots) for each stimulation frequency in (a) and (b).  $\langle \text{ISI} \rangle = \tau(1-P_{\text{fail}})$  (crimson circles). (d) The probabilities for 16 possible neuronal responses to 4 consecutive stimulations (x-axis) at 12 Hz (orange dots), where 1/0 stand for evoked spike/response failure and the theoretical probabilities assuming uncorrelated failures with  $P_{\text{fail}} \sim 0.4$  (black triangles). (e)  $P_0(m)$  at 12 Hz (orange dots). The theoretical values,  $\ln(1-P_{\text{fail}}) + m \cdot \ln(P_{\text{fail}})$  with  $P_{\text{fail}}=0.4$  (black line), similar to (c). (f)  $P_1(m)$  at 9 Hz (orange dots). The theoretical values,  $\ln(P_{\text{fail}}) + m \cdot \ln(1-P_{\text{fail}})$  with  $P_{\text{fail}}=0.15$  (black line).

A plausible biological scenario that suppresses the firing frequency of a single neuron below  $f_C$  is aperiodic time-lags between stimulations, as verified experimentally (Fig. 3(a)). For illustration, assume a slow mode of alternation between stimulation frequencies of  $2f_C$  ( $0.5\tau_C$ ) and  $2f_C/3$  ( $1.5\tau_C$ ), such that  $\langle \tau \rangle = \tau_C$ . For the high [low] frequency mode, the expected  $P_{\text{fail}}=0.5[=0]$ . Consequently,  $\langle \text{ISI} \rangle = 0.5(1.5\tau_C + \tau_C) = 1.25\tau_C$ , corresponding to a lower firing rate,  $0.8f_C$ .

The fairly good agreement between the lowered firing rate, below  $f_C$ , and the predicted one (Fig. 3(a)) strongly indicates fast neuronal plasticity (adaptation). To quantify its time scale, a neuron characterized by  $f_C \sim 5.5$  Hz was repeatedly stimulated with 200 recurrences of 80 stimulations, 40 at 12 Hz and 40 at 7 Hz (Fig. 3(b), inset). The measured  $P_{\text{fail}}$ , consists of two semi-stationary values,  $\sim 0.6$  and  $\sim 0.3$  corresponding to 12 and 7 Hz (Fig. 3(b)). The transient times between these values were found to vary among neurons between three and dozen stimulations. Quantitatively,  $P_{\text{fail}}$  (Fig. 3(b)) was fitted to the function

$$P_{\text{fail}}(i) = A \sum_{m=i-80}^{i-1} \left( \frac{\tau_C - \tau_{(m)}}{\tau_C} \right) \cdot e^{-\alpha(i-m)} \quad (1)$$

where  $i$  is an integer in the range  $[0,79]$ ,  $\tau_{(m)}$  is the time-lag between stimulations  $m$  and  $m+1$ , a negative  $m$  reads as  $\tau_{(m+80)}$  and the term  $(\tau_C - \tau_{(m)})/\tau_C$  represents the probability for a response failure following  $\tau_{(m)}$ . The last term represents the weighted exponential decay function with the optimized fitted fading coefficient  $\alpha$  (Fig. 3(b)) and  $A$  is the normalization coefficient setting  $P_{\text{fail}}(i)=1$  if all  $\tau_{(m)}$  are zero[20]. This quantitative modeling of short-term plasticity enables the examination of its abundant cooperative effects within neuronal chains and networks.

We experimentally examined a chain of two neurons, characterized by  $f_C=7.5$  and 15.5 Hz (Fig. 3(c)). The first neuron was stimulated with random  $\tau$  taken from  $U(20,110)$  ms (Fig. 3(c)), resulting in a  $\sim 7.3$  Hz average firing rate, close to its  $f_C$ , and consequently  $\sigma \sim 350$   $\mu\text{s}$  (Fig. 3(c)). The second neuron is stimulated by the first neuron at  $\sim 7.3$  Hz ( $\langle f_C \rangle = 15.5$  Hz), hence, it relays the stimulations as evoked spikes with  $P_{\text{fail}} \sim 0$  and with supreme precision,  $\sigma \sim 40$   $\mu\text{s}$  (Fig. 3(c)).

The effect of the neuronal impedance mechanism on the network level was examined using large scale simulations of excitatory networks composed of  $N=2000$  leaky integrate and fire neurons[20], whose prototypical topology was constructed using the following two steps. Each neuron is first randomly selected to have exactly one post-synaptic and one pre-synaptic connection, and the remaining connections are then selected with a survival probability of  $0.1/N$  (Fig. 4(a)). All connections are above-threshold, delays are taken randomly from  $U(6, 9.5)$  ms and neurons are selected randomly to have either  $f_C \sim 6.66$  Hz ( $\tau_C=150$  ms) or  $f_C \sim 14.28$  Hz ( $\tau_C=70$  ms) (Fig. 4(b)).  $P_{\text{fail}}$  was implemented similar to equation (1) with  $\alpha=1.4$  [20], however results were found to be insensitive to the precise  $\alpha$ . The distribution of firing rates of the 2000 neurons was estimated after several seconds using a time window of about 50 s (Figs. 4(b)-4(e)), indicating  $\sim 5.4$  Hz averaged firing rate (Fig. 4(b)) which is

even below the minimal  $f_c=6.66$  Hz. This result is a consequence of the two abovementioned experimentally verified effects. The first, a single neuron with  $f_c=6.66$  Hz along the chain enforces all its consecutive neurons to fire no higher than this frequency. Since in a recurrent network most neurons have an ancestor neuron with  $f_c=6.66$  Hz, they are expected to lower their firing rates towards this frequency. The second effect is aperiodic time-lags between stimulations, leading to firing rates even further below  $f_c=6.66$  Hz (Fig. 4(b)).

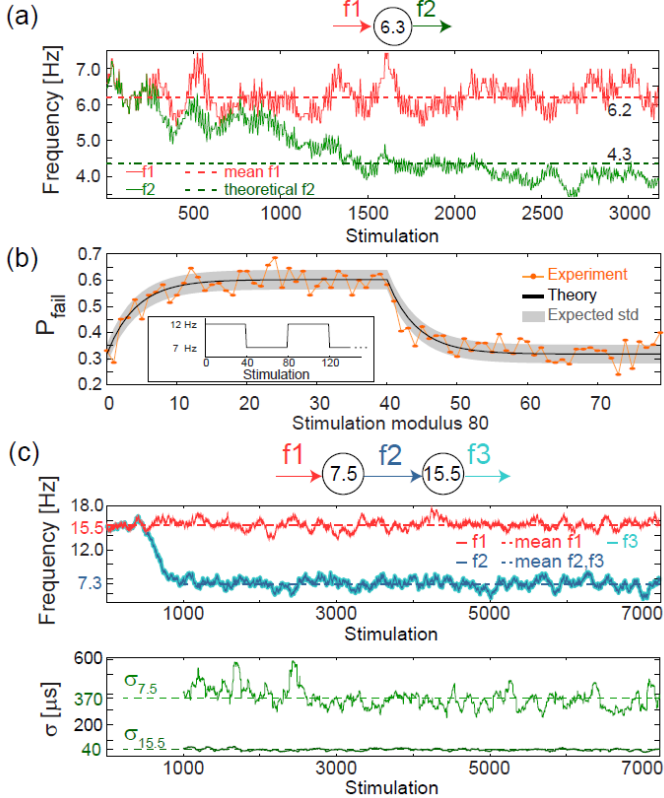


FIG. 3 (color online). (a) Schematic (top) of a neuron with  $f_c=6.3$  Hz and its stimulation/firing frequencies,  $f_1/f_2$  (red/green), respectively. The neuron is stimulated with alternating time-lags, 20 and 300 ms, ( $\langle \tau \rangle \sim \tau_c$ ), each time-lag repeating 5 to 10 times before switching.  $\langle f_1 \rangle = 6.2$  Hz (red dashed-line) is shown for comparison. The resulting firing frequency is  $\sim 4$  Hz (green full line) close to the theoretically predicted  $f_2 \sim 4.3$  Hz ( $\langle f_c \rangle$ ) (green dashed-line) following  $ISI = 0.5(160+300) = 230$  ms. (b) A neuron with  $f_c \sim 5.5$  Hz was stimulated periodically, 40 times at 12 Hz and 40 times at 7 Hz (inset).  $P_{fail}(i)$ , fitted with an optimized  $\alpha = 1.1$  following equation (1) (black line), and the expected standard deviation  $(P_{fail}(i) \cdot (1 - P_{fail}(i)) / 200)^{0.5}$  (gray area). (c) Schematic (top) of a chain of two neurons with  $f_c = 7.5$  and 15.5 Hz, their stimulation and firing frequencies. Top panel: the firing frequency of the first/second neuron (dark/light blue), obtained when the first neuron is stimulated with random  $\tau$  taken from  $U(20, 110)$  ms (red full-line). This results in  $f_2 = f_3 \sim 7.3$  Hz (blue dashed-line). Bottom panel:  $\sigma$  for the first/second neuron (light/dark green). All curves were smoothed using 100 stimulation sliding window.

The cooperative effect of the neuronal impedance mechanism drives the average firing rate of the entire network even below the lower tail of the distribution of  $f_c$ . In

this state neurons are typically in the non-chaotic phase,  $\sigma \sim 10$   $\mu$ s (Fig. 1(e)). Hence, low firing rates and  $\mu$ s neuronal precision are *simultaneously* achieved on a network level. This tendency was found to be robust to a more realistic scenario where  $f_c$  was taken randomly from  $U(6.66, 14.28)$  Hz (Fig. 4(c)). In large scale networks even lower firing rates are expected as our experiments indicate that  $f_c$  can be as low as 3 Hz, compared to the used 6.66 Hz.

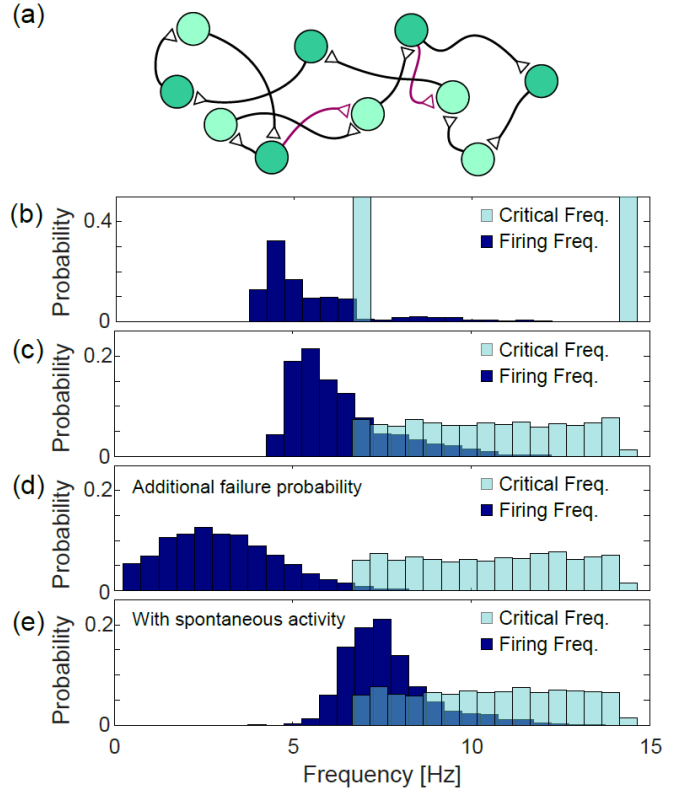


FIG. 4 (color online). (a) Schematic of the simulated networks. Each neuron has at least one randomly selected post- and pre-synaptic connection (black), supplemental connections are denoted in purple and neuronal colors stand for different  $f_c$ . (b-e) Normalized histograms of critical frequencies,  $f_c$  (light blue), and firing frequencies (dark blue) obtained in simulations for the network topology [20] (a) with  $N=2000$ . (b)  $f_c$  is either 14.28 or 6.66 Hz. (c)  $f_c$  taken randomly from  $U(6.66, 14.28)$  Hz. (d)  $P_{fail}=0.07$  is added for all firing frequencies. (e) Spontaneous stimulations are added with an average rate of 1 Hz per neuron. All results were found to be independent of the initial conditions.

The lack of response failures below  $f_c$  is too simplistic of an assumption for cortical dynamics, as failures may be generated, for instance, by synaptic noise and background inhibition. The following theoretical argument and simulations (Fig. 4(d)) indicate that indeed the proposed cooperative effect is robust to an additional response failure probability,  $p < 0.075$ , for all frequencies. The average chain length for our network topology is  $\sim 9$ , as the probability for a neuron to have two post-synaptic connections is 0.1. Consequently, the probability for an evoked spike from the last neuron in the chain, given a stimulation to the first one is

( $1-p$ )<sup>9</sup>. Since the chain terminates in a branch to two consecutive chains, the preference of spike birth over spike death requires  $2(1-p)^9 > 1$ , resulting in  $p < 0.075$ . Similarly, low firing rates on a network level were found in simulations to be robust to the scenario of spontaneous stimulations[20] (Fig. 4(e)).

This cooperative low firing rate on a network level was also found in a dense connectivity scheme where synaptic weights follow a lognormal distribution[25], as observed in some cortical networks[26]. The topology of such dense graphs does not consist of long chains; however, dynamically the firing sequences follow some preferred chain pathways.

In this work we experimentally present a biological mechanism, the intrinsic neuronal impedance mechanism, which leads to cooperation on an excitatory network, characterized by robust low firing rates. As a byproduct of these low firing rates, the nodal response timings are stabilized with  $\mu$ s neuronal precision and supporting the possibility that all building blocks of neural networks, neurons and synapses, jointly operate under the same extreme precision.

The question arises as to what functionalities demand synaptic inhibition, inhibitory links. A possible hypothesis is that stationary low firing network activity acts as a baseline cortical state. Over this state of activity meaningful neuronal functionalities are embedded by the conditional temporal formation of neuronal firing, which are an exclusive property of inhibitory synapses; probabilistically blocking an evoked spike of its driven nodes in a given time window [16]. As a result, effective spatial summations are taking place and open new routes of information flow through the network[27]. Alternatively, temporary higher frequency stimulations to a subset of neurons[28] result in abrupt changes of their NRLs[29]. The accumulation of these changes along neuronal pathways[16,17,29] temporally changes the topography of the network[16].

Technical assistance by Hana Arnon is acknowledged. This research was supported by the Ministry of Science and Technology, Israel.

[1]D. J. Amit and N. Brunel, *Cerebral Cortex* **7**, 237 (1997).  
[2]M. Shafi, Y. Zhou, J. Quintana, C. Chow, J. Fuster, and M. Bodner, *Neuroscience* **146**, 1082 (2007).  
[3]D. H. O'Connor, S. P. Peron, D. Huber, and K. Svoboda, *Neuron* **67**, 1048 (2010).  
[4]L. Daqing, K. Kosmidis, A. Bunde, and S. Havlin, *Nature Physics* **7**, 481 (2011).

[5]B. Chih, H. Engelman, and P. Scheiffele, *Science* **307**, 1324 (2005).  
[6]I. Spiegel, A. R. Mardinly, H. W. Gabel, J. E. Bazinet, C. H. Couch, C. P. Tzeng, D. A. Harmin, and M. E. Greenberg, *Cell* **157**, 1216 (2014).  
[7]T. Vogels, H. Sprekeler, F. Zenke, C. Clopath, and W. Gerstner, *Science* **334**, 1569 (2011).  
[8]A. A. Rad, I. Sendiña-Nadal, D. Papo, M. Zanin, J. M. Buldu, F. del Pozo, and S. Boccaletti, *Physical review letters* **108**, 228701 (2012).  
[9]M. Diesmann, M.-O. Gewaltig, and A. Aertsen, *Nature* **402**, 529 (1999).  
[10]D. A. Butts, C. Weng, J. Jin, C.-I. Yeh, N. A. Lesica, J.-M. Alonso, and G. B. Stanley, *Nature* **449**, 92 (2007).  
[11]S. Panzeri, N. Brunel, N. K. Logothetis, and C. Kayser, *Trends in neurosciences* **33**, 111 (2010).  
[12]M. W. Doyle and M. C. Andresen, *Journal of Neurophysiology* **85**, 2213 (2001).  
[13]A. Rodríguez-Moreno, M. M. Kohl, J. E. Reeve, T. R. Eaton, H. A. Collins, H. L. Anderson, and O. Paulsen, *The Journal of Neuroscience* **31**, 8564 (2011).  
[14]Z. F. Mainen and T. J. Sejnowski, *Science* **268**, 1503 (1995).  
[15]A. Foust, M. Popovic, D. Zecevic, and D. A. McCormick, *The Journal of Neuroscience* **30**, 6891 (2010).  
[16]R. Vardi, S. Guberman, A. Goldental, and I. Kanter, *Europhysics Letters* **103**, 66001 (2013).  
[17]R. Vardi, A. Goldental, S. Guberman, A. Kalmanovich, H. Marmari, and I. Kanter, *Frontiers in Neural Circuits* **7** (2013).  
[18]R. Vardi, R. Timor, S. Marom, M. Abeles, and I. Kanter, *Europhysics Letters* **100**, 48003 (2012).  
[19]R. De Col, K. Messlinger, and R. W. Carr, *J. physiology* **586**, 1089 (2008).  
[20]See Methods.  
[21]H. Marmari, R. Vardi, and I. Kanter, *EPL (Europhysics Letters)* **106**, 46002 (2014).  
[22]K. S. Cole, *Membranes, ions, and impulses: a chapter of classical biophysics* (Univ of California Press, 1968), Vol. 5.  
[23]J. Lübke, H. Markram, M. Frotscher, and B. Sakmann, *J. Neurosci.* **16**, 3209 (1996).  
[24]S. Boudkkazi, L. Fronzaroli-Molinieres, and D. Debanne, *J. Physiol.* **589**, 1117 (2011).  
[25]J.-n. Teramae, Y. Tsubo, and T. Fukai, *Scientific reports* **2** (2012).  
[26]S. Song, P. J. Sjöström, M. Reigl, S. Nelson, and D. B. Chklovskii, *PLoS biology* **3**, e68 (2005).  
[27]P. C. Ivanov and R. P. Bartsch, in *Networks of Networks: The Last Frontier of Complexity* (Springer, 2014), pp. 203.  
[28]S. D. Reis, Y. Hu, A. Babino, J. S. Andrade Jr, S. Canals, M. Sigman, and H. A. Makse, *Nature Physics* (2014).  
[29]R. Vardi, H. Marmari, and I. Kanter, *Phys Rev E* **89**, 042712 (2014).

## Methods

**Culture preparation.** Cortical neurons were obtained from newborn rats (Sprague-Dawley) within 48 h after birth using mechanical and enzymatic procedures. All procedures were in accordance with the National Institutes of Health Guide for the Care and Use of Laboratory Animals and Bar-Ilan University Guidelines for the Use and Care of Laboratory Animals in Research and were approved and supervised by the Institutional Animal Care and Use Committee. The cortical tissue was digested enzymatically with 0.05% trypsin solution in phosphate-buffered saline (Dulbecco's PBS) free of calcium and magnesium, and supplemented with 20 mM glucose, at 37°C. Enzyme treatment was terminated using heat-inactivated horse serum, and cells were then mechanically dissociated. The neurons were plated directly onto substrate-integrated multi-electrode arrays (MEAs) and allowed to develop functionally and structurally mature networks over a time period of 2-3 weeks *in vitro*, prior to the experiments. Variability in the number of cultured days in this range had no effect on the observed results. The number of plated neurons in a typical network was in the order of 1,300,000, covering an area of about 380 mm<sup>2</sup>. The preparations were bathed in minimal essential medium (MEM-Earle, Earle's Salt Base without L-Glutamine) supplemented with heat-inactivated horse serum (5%), glutamine (0.5 mM), glucose (20 mM), and gentamicin (10 g/ml), and maintained in an atmosphere of 37°C, 5% CO<sub>2</sub> and 95% air in an incubator as well as during the electrophysiological measurements.

**Synaptic blockers.** All *in vitro* experiments were conducted on cultured cortical neurons that were functionally isolated from their network by a pharmacological block of glutamatergic and GABAergic synapses. For each culture 20 µl of a cocktail of synaptic blockers was used, consisting of 10 µM CNQX (6-cyano-7-nitroquinoxaline-2,3-dione), 80 µM APV (amino-5-phosphonovaleric acid) and 5 µM bicuculline. This cocktail did not block the spontaneous network activity completely, but rather made it sparse. At least one hour was allowed for stabilization of the effect.

**Stimulation and recording.** An array of 60 Ti/Au/TiN extracellular electrodes, 30 µm in diameter, and spaced either 200 or 500 µm from each other (Multi-Channel Systems, Reutlingen, Germany) were used. The insulation layer (silicon nitride) was pre-treated with polyethyleneimine (0.01% in 0.1 M Borate buffer solution). A commercial setup (MEA2100-2x60-headstage, MEA2100-interface board, MCS, Reutlingen, Germany) for recording and analyzing data from two 60-electrode MEAs was used, with integrated data acquisition from 120 MEA electrodes and 8 additional

analog channels, integrated filter amplifier and 3-channel current or voltage stimulus generator (for each 60 electrode array). Mono-phasic square voltage pulses typically in the range of [-800, -500] mV and [60, 200] µs were applied through extracellular electrodes. Each channel was sampled at a frequency of 50k samples/s, thus the changes in the neuronal response latency were measured at a resolution of 20 µs.

**Cell selection.** Each node was represented by a stimulation source (source electrode) and a target for the stimulation – the recording electrode (target electrode). These electrodes (source and target) were selected as the ones that evoked well-isolated, well-formed spikes and reliable response with a high signal-to-noise ratio. This examination was done with a stimulus intensity of -800 mV with a duration of 200 µs using 30 repetitions at a rate of 5 Hz followed by 1200 repetitions at a rate of 10 Hz.

**Data analysis.** Analyses were performed in a Matlab environment (MathWorks, Natwick, MA, USA). The reported results were confirmed based on at least eight experiments each, using different sets of neurons and several tissue cultures.

Action potentials at experiments of the real-time adaptive algorithm for the stabilization of the neuronal response latency around a predefined latency were detected on-line by threshold crossing, using a detection window of typically 2-15 ms following the beginning of an electrical stimulation.

In order to overcome the temporal precision of 20 µs determined by the maximal sampling rate, 50k Hz, of our recording device, in all experiments, except the above-mentioned adaptive algorithm, the following linear interpolation method for spike detection was used. For a given threshold crossing ( $v_{\text{threshold}}$ ), we identify the two nearby sampling points:  $(t_1, v_1)$  and  $(t_2, v_2)$  where  $v_1 \geq v_{\text{threshold}}$ ,  $v_2 < v_{\text{threshold}}$  and  $t_2 = t_1 + 20 \mu\text{s}$ . Using linear interpolation between these two sampling points, the threshold crossing time,  $t_{\text{threshold}}$ , is estimated as

$$t_{\text{threshold}} = t_1 + \frac{v_{\text{threshold}} - v_1}{v_2 - v_1} 20 \mu\text{s}$$

The neuronal response latency was then calculated as the duration from the beginning of a stimulation to  $t_{\text{threshold}}$ .

**Methods of simulation.** We simulated a network of 2000 excitatory leaky integrate and fire neurons ( $N=2000$ ). The voltage  $V_i(t)$  of neuron  $i$  ( $i \in [1, N]$ ), is given by the equation:

$$\frac{dV_i}{dt} = -\frac{V_i}{\tau} + \sum_{j=1}^{2000} J_{ji} \sum_{t' \in \text{firing times of neuron } j} \delta(t - t' - D_{ji}) + J \sum_{t' \in \text{times of external stimulations of neuron } i} \delta(t - t')$$

where  $\tau=20$  ms is the membrane time constant,  $J_{ji}$  is the connection strength from neuron  $j$  to neuron  $i$  (see

connectivity section) and  $D_{ji}$  is the time delay from an evoked spike of neuron  $j$  to the stimulation of neuron  $i$  and is randomly chosen from a flat distribution  $U(6, 9.5)$  ms. The initial voltage is  $V_i(t=0) = 0.5 \forall i$ . Integration is done using the Euler method with 0.05 ms time step.

If  $V_i$  crosses the threshold, 1, the neuron may fire (see response failure section). If the neuron fires the voltage is reset to -0.5 after a refractory period of 2 ms, in which the neuron is inactive, does not respond to new stimulations. In the case of a response failure, the voltage is set to 0.2 without a refractory period.

**Connectivity.** Initially all connections are set to zero, i.e. all  $J_{ji}=0$ . First, we go over all neurons and randomly select a post-synaptic neuron for each one. Each neuron can be selected as a post-synaptic neuron only once, and a neuron cannot be connected to itself, i.e.  $J_{ii}=0$ . As a result of this procedure each neuron has only one pre-synaptic neuron and only one post-synaptic neuron. Next, we select with a probability of  $0.1/N$  additional above-threshold connections. The strength of all above-threshold connections is set to  $J_{ji}=2$ .

**Response failure.** We define  $t(i,n)$  as the time neuron  $i$  crossed the threshold for the  $n^{\text{th}}$  time. The response failure probability for the  $n^{\text{th}}$  threshold crossing of neuron  $i$  is:

$$P_{\text{fail}}(i, n) = \frac{\sum_{k < n} \left(1 - \frac{t(i, k+1) - t(i, k)}{\tau_C(i)}\right) e^{-\alpha(n-k+1)}}{\sum_{k < n} e^{-\alpha(n-k+1)}} \quad (1)$$

where  $\alpha$  is a measure of the neuronal forgetfulness and is equal to 1.4.  $1/\tau_C(i)$  is the critical frequency,  $f_C(i)$ , of neuron  $i$ , randomly chosen for each neuron as discussed in the manuscript. Note that negative response failure is taken as zero and in the limiting case of a periodic stimulation pattern, with the frequency  $f_{\text{stim}}$ , the expected response failure is obtained,

$$P_{\text{fail}}(i, n) = 1 - \left(\frac{f_C(i)}{f_{\text{stim}}}\right) \quad (2)$$

independent of  $n$ . The simulations on a network level are found to be independent of the initial conditions, which in the presented simulations were taken as  $P_{\text{fail}}(i, 0)=0$ .

**Initial stimulations.** To start the activity of the network the following external stimulations are chosen: First we randomly generate the external stimulation times for each neuron through a Poisson process with a rate of 50 Hz. Each external stimulation has a survival probability of  $\exp(-T/200)$ , where  $T$  stands for the time of the external stimulation, measured in milliseconds. Only stimulations with  $T < 1000$  ms are taken into account, as after 1000 ms the network has a self-sustaining activity, without spontaneous firing. Results are found to be

insensitive to different initial conditions, e.g. only a single stimulation to a single neuron at time 0.

**Frequency histograms.** The firing frequency of a neuron was determined as the number of times the neuron fired between 4 and 59 seconds divided by 55 seconds. The bin size for all histograms is 0.5 Hz (Figs. 4(b)-(e)).

**Additional response failure probability.** In the simulations shown at Fig. 4(d) the response failure probability is  $C+(1-C) \cdot P_{\text{fail}}$ , where  $P_{\text{fail}}$  is given by equation (1) and  $C$  is a constant. For stimulation frequencies below  $f_C$ , the response failure probability is  $C$  as  $P_{\text{fail}}$  is zero. In the presented simulations  $C=0.07$ .

**Spontaneous activity.** In the simulations shown at Fig. 4(e) the probability for a spontaneous stimulation per integration time step is  $5 \cdot 10^{-5}$ , resulting on the average in 1 spontaneous stimulation per second for each one of the neurons.

**Biological suitability.** This model is equivalent to a seemingly more biological model, under the variable substitution  $V' = (V_{\text{threshold}} - V_{\text{stable}}) \cdot V + V_{\text{stable}}$ . The equation of the voltage,  $V'$ , becomes now

$$\frac{dV'_i}{dt} = -\frac{V'_i - V_{\text{stable}}}{\tau} + \sum_{j=1}^{2000} J'_{ji} \sum_{\substack{t' \in \text{firing} \\ \text{times of} \\ \text{neuron } j}} \delta(t - t' - D_{ji}) + J' \sum_{\substack{t' \in \text{times} \\ \text{of external} \\ \text{stimulation} \\ \text{of neuron } i}} \delta(t - t')$$

with  $V_{\text{stable}} = -70$  mV and a threshold of  $V_{\text{threshold}} = -54$  mV,  $J'_{ji} = 16J_{ji}$  and  $J' = 16J$ .